

SILKWORM (*BOMBYX MORI*) COCOON *vs.* WILD COCOON Multi-Layer Structure and Performance Characterization

by

Fu-Juan LIU^{a,b,c*}, Xi-Jia ZHANG^c, and Xin LI^d

^a National Engineering Laboratory for Modern Silk, College of Textile and Clothing Engineering,
Soochow University, Suzhou, China

^b Nantong Textile and Silk Industrial Technology Research Institute, Nantong, China

^c Xihua College, Xihua University, Jinniu District, Chengdu, China

^d Harman International Industries, Suzhou, China

^e Wujiang Dingsheng Silk Co., Ltd, Shengze, Jiangsu, China

Original scientific paper
<https://doi.org/10.2298/TSCI1904135L>

*As protective shells for their biological functions against environmental damage and attack by natural predators, the silkworm (*Bombyx mori*) cocoon and its wild partner have distinctive multi-layer structures, which are systematically studied in this paper by the SEM, the thermogravimetric analyzer, and the Fourier transform infrared spectroscopy. Their mechanical properties are also investigated for the whole hierarchy and each cascade as well. In order to better demonstrate the superior survivability of cocoons in harsh environments, air permeability and moisture vapor transmission rate of the silkworm cocoon are tested. The results show the silkworm cocoons have excellent air permeability and moisture vapor transmission rate. A better understanding of different cocoons' bio-functions will be of particular importance to design thermal textiles and provide better comfort and safety for clothing in future.*

Key words: silkworm cocoon, multi-layer structure, wild cocoon, fractal calculus

Introduction

Many insect larvae spin silky cocoons for pupation. Cocoons protect pupae from predation and microbial degradation and prevent dehydration during metamorphosis [1-3]. Silkworms spin cocoons at the final larval stage. After finding a suitable place, silkworm larvae construct a loose scaffold silk and then spin cocoons that are firmly attached to a substrate by scaffold silk [4, 5].

Silkworm fibers are outstanding natural materials that have long been used for textiles. Silk-based materials have recently found applications in a growing number of areas including biodegradable medical scaffolds, implantable functional devices and tissue products. While the properties of silk fibers and silk proteins have been extensively studied [6, 7], there are substantial knowledge gaps in understanding how a wild silkworm cocoon provides the essential survival utility for the pupa residing inside. In the wild environment, a thin and light-weight cocoon can protect the silkworm from predator attacks and extreme weather conditions, while supporting its metabolic activity. As a fine product of these fully developed processes, silkworm cocoon provides strong protection against both natural predators, environ-

* Corresponding author, e-mail: liufujuan@suda.edu.cn

mental and physical adversaries, including extreme environmental temperature, during the immobile phase of life cycle when the silkworm enters diapause and metamorphosis [8]. Compared with domestic species, wild cocoons reared in an open environment require much higher level of protection. Understanding the relations between structure, property and function of this important biological material will provide a conceptual platform to design and develop novel bio-inspired textiles for thermal regulation applications. Our previous work has shown that a new fractional derivative model was suitable for explaining the excellent thermal protection of insulation clothings with cocoon-like porous structure [9, 10]. In addition, we also developed a thermal model to explain cocoon thermal regulation for pupa [11]. Now fractal calculus is widely used to deal with discontinuous problems in engineering [12-16].

Here we present our investigation of silkworm cocoons and wild cocoons in terms of their multiple layer structure and their performance characterization. We believe that a solid understanding of such highly selected cocoons will be of particular importance to future design of thermal textiles and provide better comfort and safety for fabrics and clothing.

Experimental

Materials

Silkworm cocoons and wild cocoons were collected separately, and put in beakers at room temperature.

Scanning electron microscope observation

The morphology of silkworm cocoons and wild cocoons was characterized by SEM (Hitachi S-4800, Tokyo, Japan) instrument. The samples were sputter coated with a gold film before measurements.

Thermogravimetric analysis

The thermogravimetric analyzer (TGA) was measured by the American Company Diamond Corporation's thermo differential thermal analyzer (TG/DTA). The samples were heated at 10 °C per minute in a nitrogen atmosphere with a temperature control range from room temperature to 600 °C.

Fourier transform infrared spectroscopy

Fourier transform infrared spectroscopy (FTIR) was measured using the United States NicoLET5700 infrared spectrometer. In this test, we needed to collect 1-2 mg cocoon samples, and cut them into powder which was mixed with about 200 mg KBr powder. The mixture was fully ground and then became thin slices through the compression method, and it was necessary to dry the sample again for reducing the interference of water vapor absorption. Finally, the drying tablets were put into the infrared spectrometer for testing.

Mechanical property tests of cocoons and layers

The mechanical properties were carried out by equilibrating the cocoons for 24 hours at constant temperature and humidity (temperature 20±2 °C, relative humidity 65±2%) and then performed on the Instron 3365 Universal Power Meter (Instron, USA). The test conditions were a clamping length of 10 mm, a pre-tension of 0.2 cN and a tensile rate of 10 mm per minute, respectively.

Air permeability test

Air permeability (AP) of the cocoons was performed using a SDL Atlas M021A AP tester. The test conditions were kept at the pressure of 100 Pa and the area of 20 cm², separately.

Moisture vapor transmission rate test

Moisture vapor transmission rate (MVTR) of the samples was carried out by a SDL Atlas M261 water vapor permeability tester. The test conditions were sample surface area of 28.3 cm², temperature of 37.6 °C, humidity of 50%, air flow rate of 0.3 m/s, air pressure of 1013.9 mbar, separately.

Results and discussion

Morphology

Figure 1 shows the appearance of a wild cocoon and a silkworm cocoon. The wild cocoon displays a light-yellow color. The silkworm cocoon shows white. The size of the wild cocoon is smaller. In addition, the cocoon thickness is thinner than that of the silkworm cocoon.

In order to observe the micro-structures, we performed stratification on the cocoons. However, we found that it was difficult to separate the wild cocoons, so we only peeled the silkworm cocoon wall. Although it has a 3-D non-woven structure that is made from a single continuous strand, silkworm cocoon also possesses a multi-layer structure. The inter-layer bonding is much weaker than the intra-layer bonding, which makes it easy to separate individual cocoon layers. Figure 2 exhibits the graded morphologies of cocoon in different layers throughout the thickness of a cocoon wall. From the inner to outer surface, the porosity increases while the amount of bonding between fibers decreases. The closer to the inner layer, the more significant the bonded network formed among the fibers due to the sericin coverage. The SEM micrographs of wild cocoon layers for the innermost and outermost are displayed in fig. 3. It is found that the outer layer of the cocoon has less fiber bonding than the inner layer, which is the same as that of the silkworm cocoon.

Thermogravimetric analysis

The wild cocoon and silkworm cocoon were characterized using TGA, curves (1) and (2) in fig. 4. From fig. 4, it can be seen that the weight loss curves of these two kinds of cocoons are basically the same, indicating that the chemical composition of these two kinds of cocoons are very similar.

Fourier-transform infrared spectroscopy

Figure 5 exhibits the infrared spectra of a wild cocoon (1) and a silkworm cocoon (2). From fig. 5 we find that there is no obvious difference in peak position and peak intensity, which shows again that the chemical composition of these two cocoons is similar. This result is consistent with that of the previous TGA.

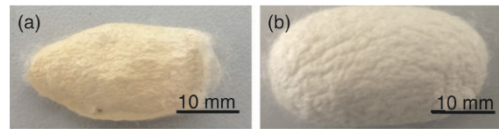


Figure 1. The pictures of a wild cocoon (a) and a silkworm cocoon (b)

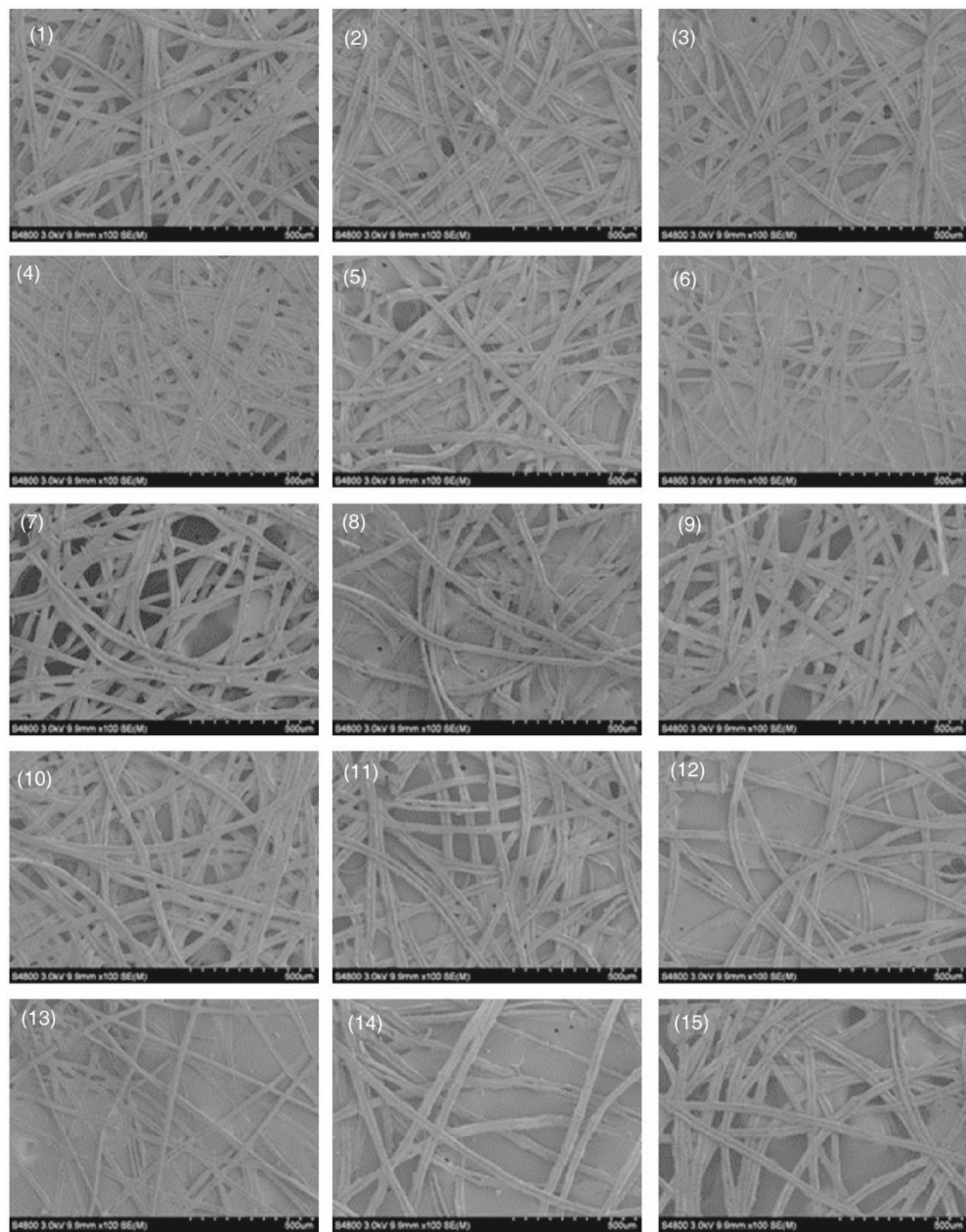


Figure 2. The SEM micrographs ($\times 100$) of silkworm cocoon layers from inner (1) to outer (15)

Mechanical properties

Due to the small number of wild cocoons and the difficulty in making test samples, we only performed mechanical properties, AP, and MVTR for silkworm cocoons. Although the silkworm cocoon was peeled into 15 layers, as shown in fig. 2, it was very difficult to test the mechanical property of each layer. Therefore, we tested the mechanical property in

every three layers from the inside to the outside. Because the porosity ranged from being highest at the outer surface and decreased into the interior, we would have expected a general modulus and strength decrease from the inside to outside layers. Figure 6 shows that a simple comparison of the stress-strain curves of every three layers from inner to outer side of cocoon. It is observed that layer 1-3 exhibits the highest Young's modulus and layer 13-15 the lowest compared to the other layers. In addition, layer 1-3 has a much higher fracture stress (33.8 MPa) and lower elongation at break (11.8%) than which layer 13-15 has (fracture stress is 12.6 MPa, and elongation at break is 26.3%). Furthermore, the fracture stress and elongation at break of the middle silkworm layers are found between the outer layers and the inner ones.

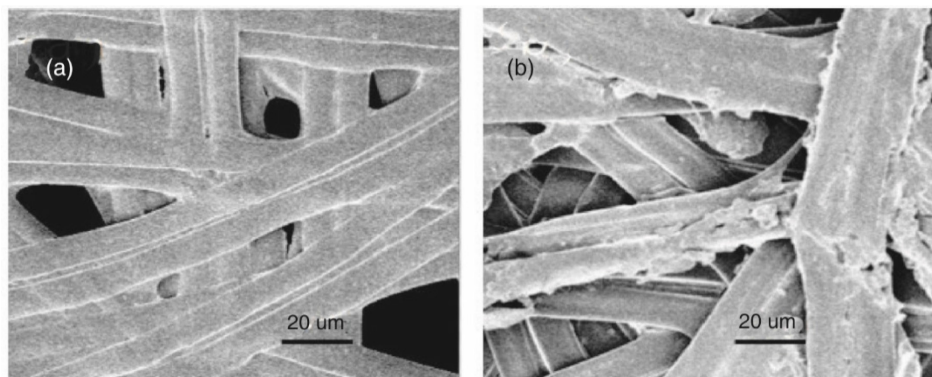


Figure 3. The SEM micrographs ($\times 1000$) of wild cocoon layers for the innermost (a) and outermost (b)

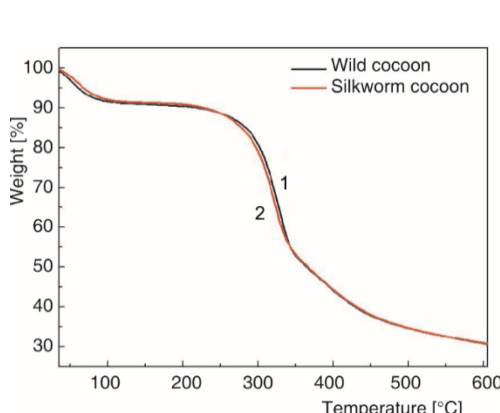


Figure 4. The TGA profiles of a wild cocoon (1) and a silkworm cocoon (2)

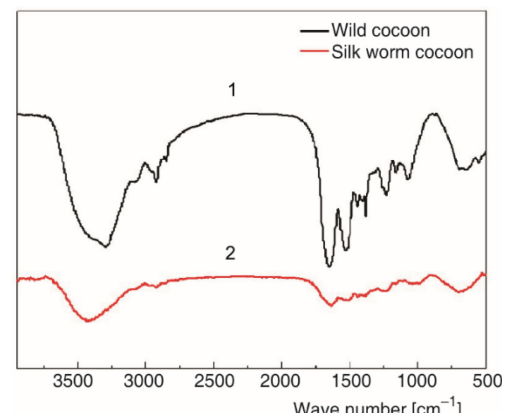


Figure 5. The FTIR spectra of a wild cocoon (1) and a silkworm cocoon (2)

The general shape of stress-strain curves of samples taken from a whole cocoon wall is similar to that of samples taken from every three layers, as shown in fig. 7. Due to individual differences, there is a clear difference in fracture stress and elongation at break of individual silkworm cocoon.

Air permeability analysis

We selected three groups of silkworm cocoons for AP. The five different locations of each group were tested and then averaged as shown in tab. 1. It is found that silkworm cocoon has excellent AP compared with the electrospinning membranes [17].

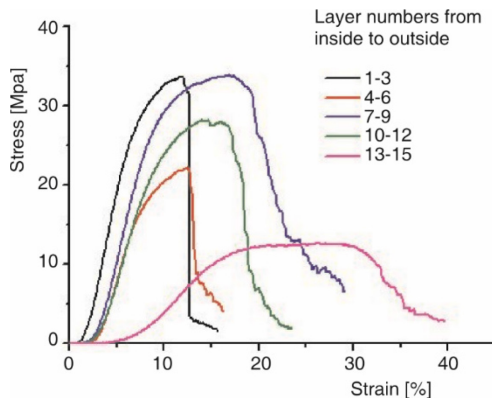


Figure 6. Mechanical properties of silkworm cocoon layers with different split numbers: stress vs. strain curves of every three layers from inner to outer side of cocoon (for colour image see journal web site)

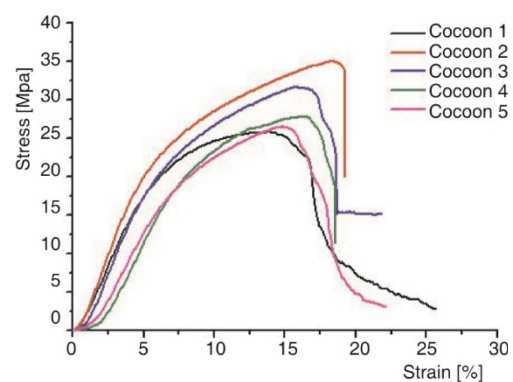


Figure 7. Mechanical properties of silkworm cocoons without split: stress vs. strain curves of five individual cocoon walls (for colour image see journal web site)

Table 1. The AP of silkworm cocoon [mms^{-1}]

| Samples \ Times | 1 | 2 | 3 | 4 | 5 | Average value |
|-----------------|-----|-----|-----|-----|-----|---------------|
| A | 232 | 213 | 234 | 209 | 206 | 218.8 |
| B | 222 | 236 | 212 | 195 | 209 | 214.8 |
| C | 205 | 213 | 217 | 212 | 203 | 210 |

Moisture vapor transmission rate

Based on the previous results of AP, we expect that the moisture vapor transmission of silkworm cocoons is also very good. Figure 8 illustrates the moisture vapor transmission curves of silkworm cocoons. Three cocoons were measured under the same test conditions. From fig. 8 we find that the three moisture-permeable curves have basically the same trend and the data are similar. As time goes by, the silk can also absorb moisture besides the moisture vapor transmission of silkworm cocoons. Therefore, in order to make the results more accurate, only the first three points of each sample are selected to study and take the average. The values of MVTR are obtained to be 1270.80, 1311.85, and 1322.13 g/m^2 per day, separately. This result shows the moisture vapor transmission of silkworm cocoons is excellent, which is better than that of electrospinning membranes [18].

Conclusions

In this work, we investigated the morphological structure and component contents, mechanical properties, air permeability, and moisture vapor transmission rate of silkworm cocoons and wild cocoons. It shows that the porosity increases while the amount of bonding be-

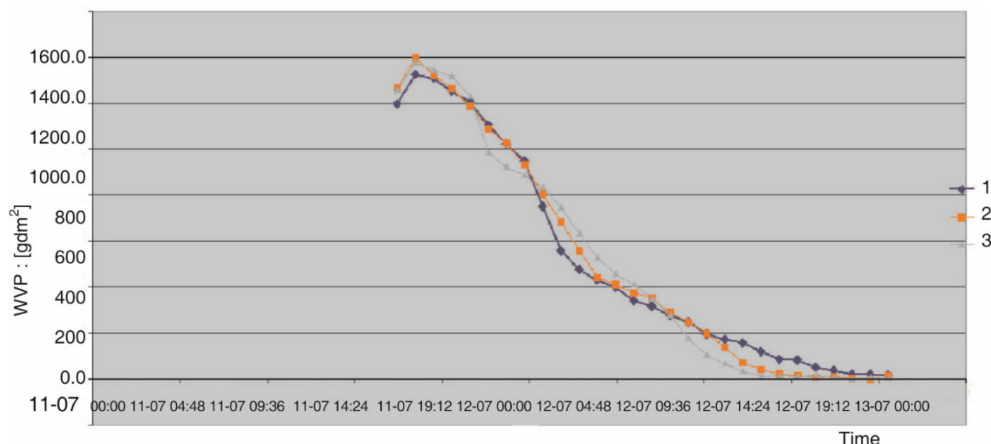


Figure 8. Moisture vapor transmission curves of silkworm cocoons

tween fibers decreases from the inner to the outer surface. The chemical composition of the two kinds of cocoons are very similar. In addition, the inner layers have a much higher fracture stress and lower elongation at break than that of outer layers for silkworm cocoons. Air permeability and moisture vapor transmission rate of silkworm cocoons are shown to be more excellent compared with that of electrospinning membranes [19-25], a math-biomimicking method was proposed in [25], and the new macromolecular electrospinning [25-27] is a promising technology to mimic cocoon structure to fabricate nanoscale artificial hierarchy in future, which has some special properties, for example, extremely high permeability, due to extremely high geometrical potential or surface energy [28-31].

Acknowledgment

This research was funded by China Postdoctoral Science Foundation (Grant No. 2017M621817), PAPD (Priority Academic Program Development of Jiangsu Higher Education Institutions), Nantong Science and Technology Project (Grant No. GY12016034), and National Natural Science Foundation of China under Grant No. 51463021.

References

- [1] Weisman, S., et al., An Unlikely Silk: the Composite Material of Green Lacewing Cocoons, *Biomacromolecules*, 9 (2008), 11, pp. 3065-3069
- [2] Gauthier, N., et al., The Acrolepiopsis Assectella Silk Cocoon: Kairomonal Function and Chemical Characterization, *Journal of Insect Physiology*, 50 (2004), 11, pp. 1065-1074
- [3] Akai, H., Anti-Bacteria Function of Natural Silk Materials, *Int. J. Wild Silkmoth Silk*, 3 (1997), Jan., pp. 79-81
- [4] Takasu, Y., et al., Identification of Ser2 Proteins as Major Sericin Components in the Non-Cocoon Silk of *Bombyx Mori*, *Insect Biochemistry and Molecular Biology*, 40 (2010), 4, pp. 339-344
- [5] Kludkiewicz, B., et al., Structure and Expression of the Silk Adhesive Protein Ser2 in *Bombyx Mori*, *Insect Biochemistry and Molecular Biology*, 39 (2009), 12, pp. 938-946
- [6] Jin, H. J., Kaplan, D. L., Mechanism of Silk Processing in Insects and Spiders, *Nature*, 424 (2003), 6952, pp. 1057-1061
- [7] Altman, G. H., et al., Silk-Based Biomaterials, *Biomaterials*, 24 (2003), 3, pp. 401-416
- [8] Roy, M., et al., Carbondioxide Gating in Silk Cocoon, *Biointerphases*, 7 (2012), 1, pp. 1-11
- [9] Liu, F. J., et al., A Fractional Model for Insulation Clothings with Cocoon-Like Porous Structure, *Thermal Science*, 20 (2016), 3, pp. 779-784
- [10] He, J.-H., A New Fractal Derivation, *Thermal Science*, 15 (2011), Suppl. 1, pp. S145-S147

- [11] Liu, F. J., et al., A Delayed Fractional Model for Cocoon Heat-Proof Property, *Thermal Science*, 21 (2017), 4, pp. 1867-1871
- [12] Li, X. X., et al., A Fractal Modification Of The Surface Coverage Model For An Electrochemical Arsenic Sensor, *Electrochimica Acta*, 296 (2019), Feb., pp. 491-493
- [13] Wang, Q. L., et al., Fractal Calculus and its Application to Explanation of Biomechanism of Polar Bear Hairs, *Fractals*, 26 (2018), 6, ID 1850086
- [14] He J.-H., Fractal Calculus and its Geometrical Explanation, *Results in Physics*, 10 (2018), Sept., pp. 272-276
- [15] Wang, Y., Deng, Q., Fractal Derivative Model for Tsunami Travelling, *Fractals*, On-line first, <https://doi.org/10.1142/S0218348X19500178>
- [16] Wang, Y., An, J.Y., Amplitude-Frequency Relationship to a Fractional Duffing Oscillator Arising in Microphysics and Tsunami Motion, *Journal of Low Frequency Noise, Vibration & Active Control*, On-line first, <https://doi.org/10.1177/1461348418795813>
- [17] Zhao, C. C., et al., Adhesion and Protective Properties of Electrospun PVA/ES Composites Obtained by Using Spiral Disk Spinnerets, *Textile Research Journal*, 87 (2017), 14, pp. 1685-1695
- [18] Vitchuli, N., et al., Multifunctional ZnO/Nylon 6 Nanofiber Mats by an Electrospinning-Electrospraying Hybrid Process for Use in Protective Applications, *Science and Technology of Advanced Materials*, 12 (2011), 5, ID 055004
- [19] Yu, D. N., et al., Snail-Based Nanofibers, *Mater. Lett.* 220 (2018), June, pp. 5-7
- [20] Liu, Y.-Q., et al., Nanoscale Multi-Phase Flow and Its Application to Control Nanofiber Diameter, *Thermal Science* 22 (2018), 1A, pp. 43-46
- [21] Liu, Y. Q., et al., Air Permeability of Nanofiber Membrane with Hierarchical Structure, *Thermal Science*, 22 (2018), 4, pp. 1637-1643
- [22] Wang, F. Y., et al., Improvement of Air Permeability of Bubbfil Nanofiber Membrane, *Thermal Science*, 22 (2018), 1A, pp. 17-21
- [23] Zhao, L., et al., Sudden Solvent Evaporation in Bubble Electrospinning for Fabrication of Unsmooth Nanofibers, *Thermal Science*, 21 (2017), 4, pp. 1827-1832
- [24] Liu, L.-G., et al., Solvent Evaporation in a Binary Solvent System for Controllable Fabrication of Porous Fibers by Electrospinning, *Thermal Science*, 21 (2017), 4, pp. 1821-1825
- [25] Tian, D., et al., Self-Assembly of Macromolecules in a Long and Narrow Tube, *Thermal Science*, 22 (2018), 4, pp. 1659-1664
- [26] Tian, D., et al., Macromolecule Orientation in Nanofibers, *Nanomaterials*, 2018, (11), 8, ID 918
- [27] Tian, D., He, J. H., Macromolecular Electrospinning: Basic Concept & Preliminary Experiment, *Results in Physics*, 11 (2018), Dec., pp. 740-742
- [28] Tian, D., et al., Geometrical Potential and Nanofiber Membrane's Highly Selective Adsorption Property, *Adsorption Science & Technology*, On-line first, <https://doi.org/10.1177/0263617418813826>
- [29] Zhou, C. J., et al., What Factors Affect Lotus Effect? *Thermal Science*, 22 (2018), 4, pp. 1737-1743
- [30] Liu, P., et al., Geometrical Potential: an Explanation on of Nanofibers Wettability, *Thermal Science*, 22 (2018), 1A, pp. 33-38
- [31] Tian, D., et al., Hall-Petch Effect and Inverse Hall-Petch Effect: A Fractal Unification, *Fractals*, 26 (2018), 6, ID 1850083